Light-adapted electroretinogram differences in Autism Spectrum Disorder

Paul A. Constable[1], Edward R. Ritvo[2], Ariella R. Ritvo[3], Irene O Lee[4], Morgan L. McNair[5], Dylan Stahl[6], Jane Sowden[7], Stephen Quinn[8], David H. Skuse[4], Dorothy A. Thompson[9,10] James C. McPartland[3]

1. Caring Futures Institute, College of Nursing and Health Sciences, Flinders University, Adelaide, Australia
2. Professor Emeritus, UCLA, Los Angeles, CA.
3. Child Study Center, Yale University School of Medicine, New Haven, CT.
4. Behavioural and Brain Sciences Unit, Population Policy and Practice Programme, UCL Great Ormond Street Institute of Child Health, University College London, London, United Kingdom.
5. Department of Psychology, Stony Brook University, New York, NY
6. School of Medicine, Washington University, St Louis, MO.
7. NIHR Great Ormond Street Hospital Biomedical Research Centre, UCL Great Ormond Street Institute of Child Health, University College London, London, United Kingdom.
8. Department of Statistics, Data Science and Epidemiology, Swinburne University of Technology, Melbourne, Australia.
9. The Tony Kriss Visual Electrophysiology Unit, Clinical and Academic Department of Ophthalmology, Great Ormond Street Hospital for Children NHS Trust, London, United Kingdom.
10. UCL Great Ormond Street Institute of Child Health, University College London, London, United Kingdom

Corresponding author
Paul.Constable@flinders.edu.au

This work was funded by research grants from the:

Alan B Slifka Foundation.

National Institute of Health U19 MH108206.

National Institute for Health Research R01 MH100173.

A generous donation from an anonymous donor in the United States of America

Key Words
Autism Spectrum Disorder, electroretinogram, b-wave, biomarker

Abstract

Light-adapted (LA) electroretinograms (ERGs) from 90 individuals with autism spectrum disorder (ASD), mean age (13.0 ± 4.2), were compared to 87 control subjects, mean age (13.8 ± 4.8). LA-ERGs were produced by a random series of nine different Troland based, full-field flash strengths and the ISCEV standard flash at 2/s on a 30 $cd.m^{-2}$ white background. A random effects mixed model analysis showed the ASD group had smaller b- and a-wave amplitudes at high flash strengths ($p<0.001$) and slower b-wave peak times ($p<0.001$). Photopic hill models showed the peaks of the component Gaussian ($p=0.035$) and logistic functions ($p=0.014$) differed significantly between groups. Retinal neurophysiology assessed by LA-ERG provides insight into neural function in ASD and represents a candidate biomarker worthy of additional study.

The retina is an accessible model of neural connectivity in the brain (Lavoie et al. 2014), and specific retinal signaling pathways can be probed and measured with an electroretinogram (ERG). The ERG records the change in voltage over time produced by the retina in response to brief flashes of light in dark- and light-adapted conditions (McCulloch et al. 2015; Robson et al. 2018). The retinal networks contributing to the ERG depend upon the ambient lighting; when dark-adapted (DA) in low light, the signal path is driven by rod photoreceptors connecting with rod ON-bipolar cells and horizontal cells, and when light adapted (LA) in bright light, the pathways are driven by cone photoreceptors that synapse with both ON- and OFF – cone bipolar cells and horizontal cells. The shape of the ERG is the sum of the relative contributions of each cell type: broadly, the first negative a-wave reflects photoreceptor hyperpolarization to light and the following positive b-wave is an index of depolarizing bipolar cells.

It is known that the shape of the ERG is altered in some neurological diseases. A recent systematic review has highlighted the growing use of the ERG in psychiatric disorders and its potential for identifying conditions based on the ERG waveform (Youssef et al. 2019). For example, schizophrenia (Hébert et al. 2015) found smaller LA a- and b-wave amplitudes as well as a prolonged b-wave peak times, and in depression (Hébert et al. 2017) reported a delayed cone b-wave time to peak. Recently, the ERG a-wave amplitudes under LA and DA conditions differentiated schizophrenia and bipolar disorder (Hébert et al. 2020). These findings indicate that the ERG is able to reveal differences in the nature of neural transmission that are governed by the same CNS neurotransmitters. The overlapping interactions of genes implicated in ASD and schizophrenia for instance (Hoerder-Suabedissen et al. 2013; Pathania et al. 2014) and similar changes of a- and b-wave amplitudes and b-wave time to peak in schizophrenia (Hébert et al. 2020) and these reported in this study, suggests that the ERG could help our understanding of a diverse range of psychiatric disorders encompassing ASD, ADHD, OCD, schizophrenia and bipolar disorder (Lavoie et al. 2014, Youssef et al. 2019). The ERG offers the potential to help our understanding of neurodevelopmental and neurodegenerative conditions as a non-

invasive and objective measure of retinal activity in response to brief flashes of light (Schwitzer et al. 2015; Lavoie et al. 2014).

Autism spectrum disorder (ASD) is a neurodevelopmental disorder defined by difficulties in social-communication, repetitive behaviors and atypical response to sensory information (APA 2013). While the etiology in most cases is unknown, both genetic and environmental factors are believed to contribute to the ASD phenotype through modulation of synaptic connectivity and regulation of neurotransmitters and their transcription factors (Autism Genome Project 2007; Chaste and Leboyer 2012; Yu et al. 2015; Doherty et al. 2018; An et al. 2018; Grove et al. 2019; Sanders et al. 2015). There are presently no biomarkers for ASD (McPartland 2016).

Differences in the ERG waveform in ASD may help our understanding of the biology of factors contributing to ASD. To date there have been only three published studies in humans about the retinal function of individuals with ASD. The first two, 30 years ago, reported a smaller DA-ERG b-wave in a large group of children with ASD (Ritvo et al. 1988) and noted differences in siblings and probands within a family (Realmuto et al. 1989). Recently, this observation was confirmed in a small group of adults with ASD (Constable et al. 2016). In addition, Constable et al. (2016) examined the LA-ERG b-wave amplitude and found it was smaller at certain flash strengths. The novel LA-ERG observations of Constable et al. (2016) are supported by evidence of altered ERGs from rodent models of neurodevelopmental disorders in ASD (Zhang et al. 2019; Guimaraes-Souza et al. 2019), Fragile X syndrome (Rossignol et al. 2014) and ADHD (Dai et al. 2017). Additional benefits of studying the LA-ERG are that the greater complexity of the cone pathways makes the LA-ERG an excellent tool for probing the detail of a retina's response to light (Lavoie et al. 2014; McCulloch et al. 2019), and, because it does not require 20 minutes adapting to darkness, the LA-ERG is a quicker and more acceptable assay than the DA-ERG.

Encouraged by this limited but accumulating evidence, the present study sought to explore the nature and frequency of differences in LA-ERGs with sufficient power in a large group of young individuals with ASD from multiple centers.

Methods

The ERG is a clinical test recorded according to an International Society of Clinical Electrophysiology of Vision (ISCEV) standard (McCulloch et al. 2015). For this study we compared the peak amplitudes and timings of the cone driven LA-ERG a- and b-waves for nine flash strengths in addition to the ISCEV standard LA 3.0 flash.

This study comparison between children and young adults with ASD and the control group was conducted across three sites based in London (UK), New Haven (USA) and Adelaide (Australia). Each study center had a study lead, and each center received local ethical approval for the study protocol. ERG recordings were taken by trained individuals at each site who were not blinded to the subject group to which the participant belonged.

Participants

ASD participants were recruited from existing clinical populations at each center based in the UK and USA and in Australia via invitations to participate in research through local autism associations and social media. All ASD participants met DSM-IV or DSM-5 criteria based on assessment with ADOS or ADOS-2 (Luyster et al. 2009) or clinical assessment by a pediatric psychologist. Participants in either group were excluded if there was a family history of ocular disease, strabismus, history of epileptic seizures in the last year, an IQ < 65 and/or were unable to follow simple verbal; instructions, had a congenital syndrome such as Fragile-X, Downs or Rett's or had any history of brain trauma or

pathology. Written informed consent was obtained from the parent/guardian, or the individual if they were older than 16 years of age. Autism Severity Scores were calculated using the methods of Gotham et al (2009). FSIQ measures were measured by WISC or WASI (Wechsler 1999, 2003) as appropriate (Table 1).

A total of 97 ASD and 90 control subjects were initially recruited for the study. In the ASD group, five were excluded due to non-compliance/poor fixation, and two were excluded due to inappropriate placement of the electrode, leaving 90 ASD participants. From the 90 control subjects, one was excluded due to non-compliance/poor fixation, and two were excluded due to inappropriate placement of the electrode, resulting in a total of 87 control participants in the study. In addition, only one eye was included in three of the ASD subjects following review of the electrode positions. Therefore, a total of 90 ASD (177 eyes – 88 left and 89 right eyes) and 87 control (174 eyes – 87 left and 87 right eyes) were included in the final analysis.

Within the ASD group, 13 had a confirmed medical comorbid diagnosis of ADHD; 1 had anorexia; 1 had OCD and Dyslexia, and 1 had developed myalgic encephalomyelitis. The mean age (sd) and range of the 177 ASD group's eyes were 13.0(4.2), 6.0 - 25.8 years, with 130 male and 47 female eyes. For the 174 control eyes, the mean age was 13.8(4.8) with a range of 5.4 - 26.6 years and with 82 male and 92 female eyes. The iris color index was computed as a ratio of the 25^{th} centile gray values obtained from two 1 mm line segments centered vertically from the pupil margin to the 25^{th} centile gray scale values of the pupil diameter. The ratio (iris color index) provided an objective measure of iris pigmentation for each eye because darker irises absorb more light and reduce the ERG waveform amplitudes (Al Abdlseaed et al. 2010). The mean iris color index was 1.26(0.12) for the control group and 1.21(0.10) for the ASD group.

The participant demographic was diverse, reflecting the study centers' population bases. The control and ASD groups were 67.2% and 80.8% Caucasian respectively, with the remaining participants originating from Asia and mixed African/Caucasian backgrounds.

In the ASD group the number of individuals and types of medications were: 12 on dopamine re-uptake inhibitors, 7 on selective serotonin reuptake inhibitors (SSRI), 6 on melatonin at night, 6 on antihistamines/asthma inhalers, 4 were taking vitamin supplements, 3 were on alpha-2 agonists or asthma inhalers, with one taking insulin for diabetes, one a proton pump inhibitor, and one who had a history of taking antiepileptic medications but none in the previous six months. In the control group one participant was taking a SSRI, and two were taking beta agonists and one used an asthma inhaler. Only four of twelve ASD participants had taken their dopamine re-uptake inhibitor on the day of testing. Dopamine antagonists can decrease the b-wave amplitude in human subjects (Holopigian et al 1994). However, interactions with dopamine and GABA are complicated by the range of different dopamine receptor subtypes expressed in the retina (Popova 2014) and in frog retina, serotonin has been shown to increase the b-wave amplitudes (Popova and Kupenova 2017).

To control for medications, and potential interactions with the ERG waveform, the results of the statistical analysis were independent of whether subjects were taking a CNS medication or not. A further sub-analysis was performed on the b-wave amplitude data excluding those on medications that had a CNS effect. In order to further control for the heterogeneity of the groups with gender and ethnicity a further homogeneous subset of data of the b-wave amplitude was analyzed which contained only individuals that were, Caucasian, male, under 16 years of age, and who had no co-morbidities such as ADHD. (See supplementary material for full results of the homogeneous analysis of b-wave amplitude).

ERG Recording Protocol

The custom Troland based, nine-step, LA full-field ERG series was performed on both eyes using white flashes and background with Commission Internationale de l´Eclairage (CIE) co-ordinates x= 0.33, y= 0.33, generated by LEDs within the Ganzfeld. Flashes of 0.4, 0.8, 1.3, 2.5, 4.0, 6.3, 8.9, 13 and 16 phot cd.s.m^{-2} were presented in random order, 2/s, on a 30 cd.m^{-2} white background and averages of 30 trials per sample were taken from each eye. The 30 cd.m^{-2} white background was chosen as this is the current recommendation for recording the LA-ERG under dilated conditions. With non-dilated pupils there is some evidence that this background luminance may shift the photopic hill to the right and that an 80 cd.m^{-2} may be preferable (Gagné et al. 2010). Liu et al. (2018) demonstrated a good positive correlation of 0.74 for the LA b-wave amplitudes between a dilated full field ERG and the Troland based undilated ERG using the RETeval device. Traces were rejected from the average if they fell above or below the 25th centile. The right eye was always recorded first within the protocol. The b-wave amplitudes were plotted against flash strength to establish the photopic hill function for each group (See Figure 2). Following the nine-step LA series a recording of the right then left eye to the ISCEV standard flash 3.0 cd.s.m^{-2} on a 30 cd.m $^{-2}$ white background at 2/s was made with 30 samples averaged to generate the waveform. Repeats of the recording were performed as required.

The RETeval (LKC Technologies Inc, Gaithersburg, MD, USA) instrument was used for all recordings. All centers used the same RETeval, make and model that were calibrated prior to use by the manufacturer. The RETeval digitally records ERGs to a pre-programed, but randomized flash sequence from a self-adhesive skin electrode positioned below the lower eyelid (See Figure 1 and supplementary video for a recording of the right and left eye). Recordings were automatically stopped by the RETeval if pupil tracking was lost (poor fixation), electrode impedance was > 5kΩ (electrode unstuck), or if pupil diameter was too small for the Troland protocol to provide the required the flash strength for any specific retinal illuminance.

Figure 1 Image of a participant eye during recording through the Ganzfeld dome of the RETeval instrument and a recording set-up with the child seated in a normally lit room. See supplementary video for recording. The electrode is visible below the eyes – placed at 2mm and contains the active, ground and reference electrode within a single skin adhesive electrode.

The participant was seated, and the skin electrode was placed 2-3mm below the lower eyelid following skin preparation if required to reduce impedance to <5kΩ in accordance with the manufacturer's instructions. The participant was instructed to look steadily at a dim red LED located in the center of the Ganzfeld dome and to try to avoid blinking or eye movements. The Troland protocol measured the pupil size continuously and automatically adjusted the flash strength in real time, negating the need to dilate the participant's pupils for the flash series. All recordings were performed under normal room lighting conditions. Recordings could be stopped and restarted to accommodate rest breaks as required. An in-built infra-red camera recorded each session so that post-analysis of electrode placement and fixation could be reviewed. Successful measurements of the a- and b-waves were achieved in the ASD group in 89.2% to 98.9% of the time and for the controls the success was slightly higher ranging from 90.3% to 100%. (See supplementary material for complete record of recorded traces).

Data Handling and Reporting

The amplitude and time of the a- and b-waves were reported automatically by an in-built algorithm and checked manually for accurate cursor placement. If the a-wave amplitude was < 1 μV, the time and amplitude were ignored for that waveform. When repeated measurements were taken, the waveform with the largest b-wave amplitude was included as the b-wave amplitude was the primary outcome measure. Raw data, video and images of the electrode below the eye and iris color index were all exported for further analyses using the RFF extractor ver 2.9.4.1 (LKC Technologies Inc, Gaithersburg, MD, USA). A sample report showing automatic cursor placement is shown in the supplementary material. We report the a- and b-wave amplitudes and their time to peak or trough as well as the b:a amplitude ratio for this LA ERG series.

The vertical and horizontal electrode position were measured from the photographic image produced of each eye during the recordings using a calibrated graticule. Electrode position can affect the amplitude of the ERG signal (Hobby et al. 2018) and eyes in which the electrode position was greater than 4mm were excluded. All images were inspected, and the position of the electrode measured with a weighting of 2mm below the eye set at zero in the statistical model.

Statistical Methods

The primary outcome is the b-wave amplitude and secondary outcomes are the time to peak of the b-wave, the a-wave amplitude and time to peak and the ratio of the b-wave amplitude to the a-wave amplitude (b:a ratio). The differences in the a- and b- wave amplitudes and timings and the b:a ratio for the nine random series flash strengths were modelled using multilevel random effects mixed models. Each subject contributed 18 observations, nine from each eye at the differing flash strengths. Eye, subject and center were nested and entered into the model as random effects to account for correlated readings. This mixed model method thus accounts for any correlation between right and left eyes of an individual and allows data from each eye to be used. The dependent variable was the b-wave amplitude, with secondary outcomes the timing of the b-wave peak, the a-wave amplitude, the time to the a-wave

minimum and the b:a wave amplitude ratio. These were compared to the 5th centile cut-off in the control population. The independent variables were age, gender, iris color index, electrode height, CNS medications, and polynomial terms in flash strength up to the fourth power and group (ASD or control). In order to model the data accurately between groups, the interaction term between group and the polynomial terms in flash strength was also entered into the model. For the ISCEV standard flash, the same mixed model was used without the main effect of flash strength and the interaction terms involving flash strength and group assignment. AIC and BIC criteria were used to assess comparative model fit. No attempt has been made to adjust for multiple comparisons, because this was an exploratory study to identify the most suitable flash strength which differentiated the groups. Two methods were used to calculate the Cohen's *d* effect sizes based on a multivariable and univariable analysis of the datasets. Within the text, the multivariable then univariable effect sizes are reported then the z-scores. A *p*-value less than 0.05 (two-tailed) was deemed to be statistically significant. The analyses were conducted using Stata 16.0 (StataCorp, College Station, Texas).

The luminance-response function, termed the photopic hill, was modelled for each group according to the method originally described by Hamilton et al. (2007) with the same assumption that n =1 for equation 1 to limit the number of free parameters (McCulloch et al. 2019). The model is the sum of a Gaussian function that represents the OFF pathway and a logistic function that represents the ON pathway. The photopic hill equation model is given by:

$$y = G_b \left[\left(\frac{I}{\mu} \right)^{\frac{\ln\left(\mu / I\right)}{B^2}} \right] + \frac{V_{b\,max} I}{I + \sigma_b},$$

where y is the b-wave amplitude (μV), measured from the trough of the a-wave, G_b is the maximal Gaussian amplitude, I is the flash strength (cd.s.m^{-2}), μ is peak flash strength, B is a measure of the width of the Gaussian curve, V_{bmax} is the maximal saturated amplitude and σ_b is the semi-saturation flash strength that evokes a half-maximal response of the b-wave amplitude. Non-linear regression (Stata's nl command), clustering over subject, was used to estimate the five parameters and compare the same parameters between groups. Parameter estimates were verified though SigmaPlot.

The photopic hill is a plot of the b-wave amplitude versus flash strength. In the LA-ERG the b-wave amplitude is a sum of the ON and OFF responses. The photopic hill is characterized by a peak then plateau with the peak being generated largely by the OFF- pathway and the plateau by the ON pathway (Hamilton et al. 2007; Lachapelle et al. 2001; McCulloch et al. 2019) because as the flash strength increases the ON response diminishes and the OFF response is delayed (Ueno et al. 2004).

Results

Group Characteristics

There was a significant difference between groups for sex (74.5% male in the ASD group compared to 47.1% in the control group, $p<0.001$) and iris color index (mean(sd), with the control group having darker irises 1.26(0.13) compared to the ASD group 1.21(0.10); $p=0.003$. (See Supplementary material for histogram of distribution of iris color indices). There were no significant differences between groups for age. The FSIQ for ASD was 99.7(16.7), and mean calibrated severity score for the ASD participants was 6.7(2.0) from a range of scores 4-10 (See Table 1 for full details).

Table 1 Participant information from the three study centers

Demographic characteristics*	**ASD†**	**CONTROL†**	**p-value‡**
n(eyes)	177	174	
Age (inter Quartile Range)	12.6(9.9-15.3)	12.8(10.1-16.6)	.12
Caucasian n(%)	143(80.8)	117(67.2)	.004
Male gender n(%)	130(74.5)	82(47.1)	<.001
Iris color index (AU)§	1.21(0.10)	1.26(0.13)	.003
Vertical position (%) 0 1 2 3 4	 2(1.1) 15(8.5) 84(47.5) 47(26.6) 29(16.4)	 0(0.0) 16(9.2) 81(46.6) 53(30.5) 24(15.1)	 .58
FSIQ†	98.9(16.5)	-	-
Autism Severity	6.3(2.6) range: 4-10	-	-

* Data reported as n(%), mean(sd) or median(lower quartile – upper quartile) as appropriate
‡P-values obtained from chi-square tests, t-tests or ranksum tests as appropriate
† ASD: Autism Spectrum Disorder, Control: Participant without ASD; FSIQ: Full Scale Intelligence Quotient.
§ AU: Arbitrary units of grey scale ratio between iris and pupil.

Photopic Hill

Figure 2 shows the plot of the ASD and control nine random step LA series with mean b-wave amplitude with 95% CI verses the flash strength in log phot cd.s.m^{-2}.

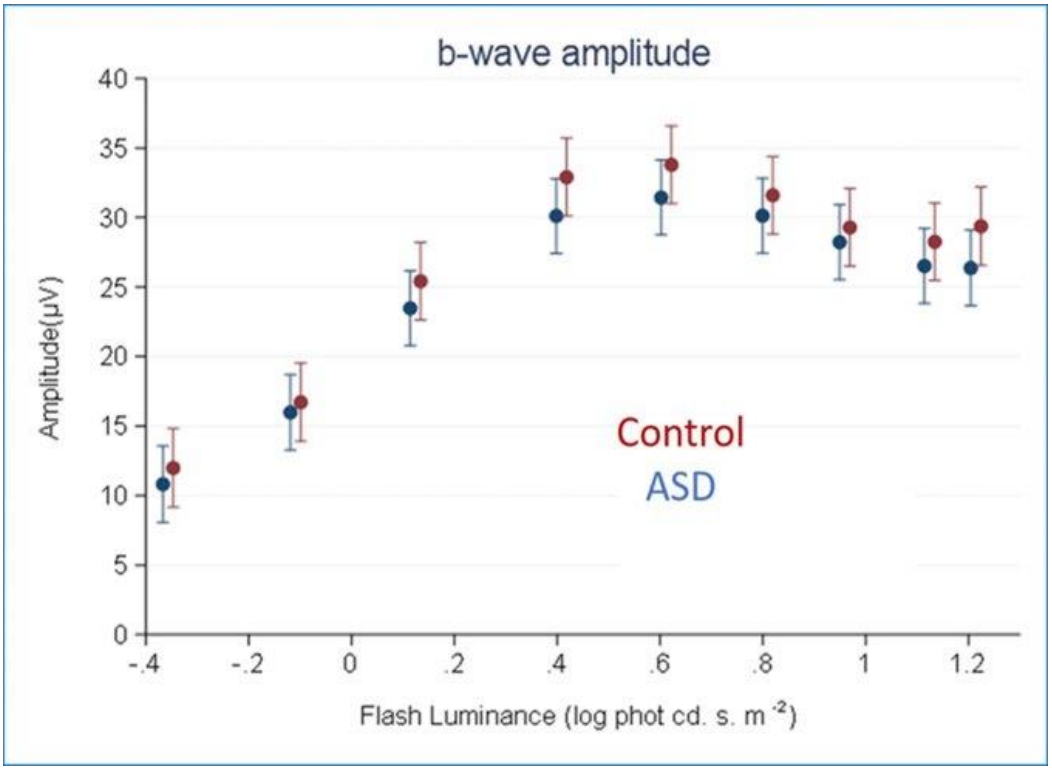

Figure 2: The amplitudes of the b-waves at the nine flash strengths eliciting the photopic hill function characterized by at peak and late plateau at the higher flash strengths. Plot shows the mean with 95% CI for ASD and Control groups. Significant values for b-wave amplitude are shown (*p< .05; **p< .01; ***p< .001).

Table 2 shows the difference in parameters estimates for both groups.

Table 2 Estimates of the photopic hill parameters.

	ASD	**CONTROL**	**p-value**
	β(95% CI)	β(95% CI)	
G_b	9.31 (8.05 – 10.58)	11.07 (10.02 – 12.11)	.035
μ	1.58 (1.56 – 1.61)	1.55 (1.53 – 1.58)	.10
B^2	0.14 (0.10 – 0.17)	0.14 (0.11 – 0.16)	.91
V_{bmax}	28.69 (27.28 – 30.11)	31.12 (29.80 – 32.45)	.014
σ	0.30 (0.27 – 0.33)	0.30 (0.27 – 0.32)	.97

Parameter values for the fitted solutions to the photopic hill model.

Modelling of the photopic hill as described resulted in significant difference for the parameters μ, V_{bmax} and B. For the control group the mean(SE) amplitude of the plateau (V_{bmax}) that follows the photopic hill peak at higher flash strengths was 31.12(0.67) μV and for the ASD group it was 28.69(0.72) μV

and representative of the ON pathway reduced contribution in the ASD group (p= 0.014). In addition, the height of the Gaussian represented by the parameter G_b and indicative of OFF pathway contribution to the photopic hill was also significantly reduced (p=0.035) in the ASD group 9.31(0.62) μV compared to 11.07 (0.53) μV for the control group. All other parameters were not significantly different (p≥.10).

The a and b-waves

Figure 3 shows a representative series of ERG waveforms produced by the ten flash strengths used; the mean group amplitudes of the a- and b-waves are reduced in the ASD compared to the control group. There were several significant differences between the groups with respect to the timing and amplitude of the b-wave and amplitude of the a-wave that occurred at flash strengths after the peak of the photopic hill above 8.9 phot cd.s.m^{-2} (0.95 log phot cd.s.m^{-2}) which is dominated by contributions of the ON pathway (See supplementary material for full table of results).

For the primary outcome of b-wave amplitude , the most significant difference between the groups was observed at the strongest flash strength at 16.0 cd.s.m^{-2} (1.2 log phot cd.s.m^{-2}) with the ASD group having a smaller amplitude: (-3.36 ± .96, p <.001) [ASD: 26.4(1.4) μV; control 29.7(1.4) μV]*d* = -.17, -.36, z = -3.49. For the secondary outcomes, a-wave amplitude, the most significant group difference occurred at the second highest flash strength at 13 cd.s.m^{-2} (1.1 log phot cd.s.m^{-2}) with the ASD group recording lower amplitudes (-1.00 ± 0.24, p=.000) [ASD:8.9(0.4) μV; control 9.9(0.4) μV], Cohen's *d* = -.19, -.31z = -4.13 . For the secondary outcome of the b-wave time to peak, the greatest difference between the groups was observed at the third strongest flash strength at 8.9 cd.s.m^{-2} (0.95 log phot cd.s.m^{-2}) with the ASD group showing a slower time to peak: (+0.36 ± .11, p <.001) [ASD: 29.6(0.1); control 29.3(0.1) ms], Cohen's *d* = .23, .32, z = 3.17 . At this strength the b:a ratio was also significantly smaller in the ASD group (-0.40 ± 0.15, p=.007), Cohen's *d* = .19, .33, z = 3.30.

The a-wave time to peak was not significantly different between groups (p =0.11) and the ISCEV standard flash (3 cd.s.m$^{-2)}$ at 85 Td.s also did not reach significance across the parameters (p≥0.06). (See supplementary material for full table of results).

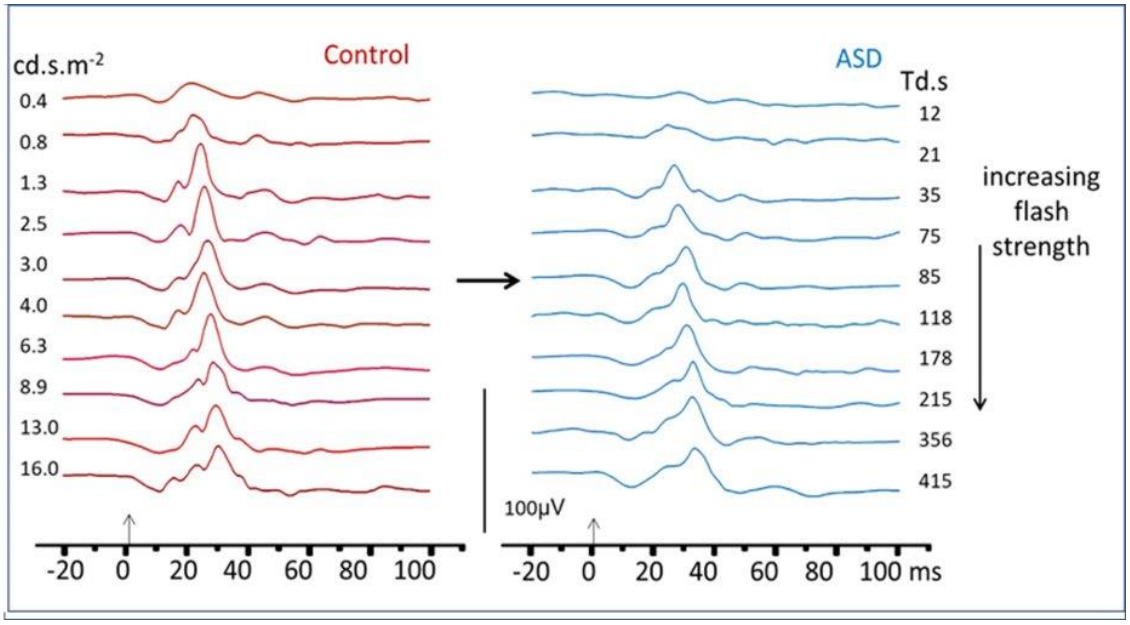

Figure 3 Representative raw traces of ERGs produced by the 10 flash strengths used in this study. Arrow indicates the standard ISCEV LA3 ERG. Flash strength increases from top to bottom.

Homogeneity

A further sub-analysis was performed on the b-wave amplitudes in those not taking any CNS medications to exclude the possibility that the findings were related to therapeutic actions of the medications on the retina. When participants taking CNS acting medications were excluded then there remained a significant group difference at log 1.2 log phot cd.s.m^{-2} (p=.003, z= -3.02).

When we analyzed a more homogeneous sub-set of the populations so that all were male, Caucasian, aged under 16 years of age and taking no CNS medications and for the ASD group only those with a single diagnosis of ASD without any comorbidities such as ADHD. Then the b-wave amplitude differences were more significant than in the larger and broader more heterogeneous group. For the b-wave amplitude at 1.2 log phot cd.s.m^{-2} the ASD group (n=63 eyes aged 11.6 (2.4) were significantly smaller, (-6.91 ± 1.64, p<.001) [ASD:25.5(1.8) µV; compared to the control (n=41 eyes, aged 11.9 (2.8) years) with a b-wave amplitude of 32.5(2.0) µV] z=4.21.

Sensitivity and Specificity

To assess the ability of the b-wave amplitude to discriminate between groups the RoC plots were generated for the whole group and for those less than 16 years of age at 16 cd.s.m^{-2} (log 1.2 phot cds.m^{-2}). For the subset of participants aged less than 16 years the AUC was 0.723 (sensitivity = 70.1%, specificity = 59.4% at cut-off = 0.425)and was comparable to the AUC for all participants with an AUC of 0.740 (sensitivity = 70.7%, specificity = 65.7% at cut-off = 0.5), indicating that the age of the participant's did not have an effect on the sensitivity or specificity of the b-wave amplitude to differentiate between groups (See supplementary material for RoC curves). There was no significant correlation with ASD severity scores (Spearman's rho = -0.067, p=.26) or ADOS total scores (Spearman's rho = -0.213, p=.28).

Discussion

The main finding is that the primary outcome, the LA ERG b-wave amplitude was reduced in the ASD group. For the secondary outcomes, the b-wave time to peak and a-wave amplitude were delayed and reduced at the higher flash strengths respectively, along with a reduced b:a wave amplitude ratio. The modelling of the photopic hill found a group difference in the contributions of both the ON and OFF pathways that summate to produce the b-wave. Although the ON- component V_{bmax} showed a more significant difference than the OFF-component G_b, both were affected, implicating a difference in the way cone and bipolar cells connect and/or communicate in ASD.

The ERG waveform is produced by the summation of negative and positive voltage changes in the retina with the maturation of the b-wave following the a-wave. The a-wave is largely due to hyperpolarization of the photoreceptors, with a partial contribution of OFF bipolar cells (Ueno et al. 2004). The b-wave of the LA-ERG develops as a result of depolarization of the ON-bipolar cells

followed by depolarization of the OFF bipolar cells at the end of the flash. In addition, lateral inhibitory currents are also present from horizontal cells that share the cone synapse with the bipolar cells (Chapot et al. 2017). Amacrine cells located in the proximal retina contribute to the early OPs inhibitory circuits to the ON pathway with the later OPs associated with the OFF pathway through local circuits (Wachtmeister 1998). The timing of the peak and trough of the b- and a-waves is an interactive relationship, as the recorded waveform is the result of the summation of two temporally overlapping events with the b:a wave amplitude representing this relationship.

Therefore, there are multiple levels at which the b-wave could be affected through interactions with neuronal circuits and synapses within the retina. However, the photopic hill models show that both the ON and OFF pathways are altered suggesting generalized dysfunction at the synapse that is formed between one cone with one ON-and one OFF-bipolar cell and one horizontal cell. This synaptic triad is regulated by glutamate signaling between the cone and bipolar cells and the inhibitory GABA neurotransmitter from horizontal cells between the cone and horizontal cells (Thoreson and Mangel 2012).

All retinal bipolar cells use glutamate as the neurotransmitter between the photoreceptor and bipolar cells. The ON- bipolar cells use metabotropic glutamate receptors- primarily mGLUR6, and the OFF bipolar cells use the ionotropic glutamate receptors – primarily GLUR4 (Hanna and Calkins 2007). With the ON-bipolar cells depolarizing at the onset of a light increment (at flash onset) and the OFF bipolar cells depolarizing at the end of the flash interval (at flash offset) separated by 2-3 ms there is a temporally overlapping contribution of ON and OFF bipolar cells to the overall timing of the b-wave peak and its amplitude depending upon the dynamics of these glutamate synapses. The findings of differences in the timing and amplitude of the b-wave under LA conditions could also be explained by a dysfunction of the kinetics and/or expression levels of the receptors found at the cone-bipolar-horizontal cell synapse changing the overlapping timings and amplitude peaks generated at this first

retinal synapse (Robson et al. 2018; Chapot et al. 2017). Given both glutamate and GABA have been implicated in ASD, with genetic differences in receptors and transporters of these neurotransmitters, an imbalance of these neurotransmitters in the retina may reflect parallel imbalances in the ASD cortex (Coghlan et al. 2012; Fatemi and Folsom 2015; Pizzarelli and Cherubini 2011; Gadow et al. 2010; Hadley et al. 2014; Uzunova et al. 2014). Whilst abnormalities in glutamate receptor expression may explain the findings in ASD, there are possibilities that glutamate transporters and regulators of neuronal development, such as fragile-X mental retardation protein (FMRP) or mGLUR5, which regulates FMRP expression, may also be involved. Recent studies in a rodent model of ASD (Guimaraes-Souza et al. 2019) found approximately 1.5 x more expression of FMRP and mGLUR5 proteins in the outer and inner plexiform layers which may contribute to an altered signaling between neurons in the outer and inner retina.

The photopic hill describes the pattern of amplitude changes in the LA-ERG b-wave as flash strength increases. Initially b-wave amplitude grows, but, at higher strengths, it decreases to a plateau and shows a 'hill' profile. The photopic hill is due to an interaction of ON and OFF pathways that are differentially altered by flash strength (Ueno et al. 2004). The findings that the parameters that model the ON- and OFF-bipolar cell contribution indicate a difference in the signaling along these pathways. However, it is also possible that the reduced b-wave amplitudes may in part be the result of amacrine cell circuits that contribute to the b-wave (Wachtmeister 1998). The oscillatory potentials (OPs) when examined in the original study by Constable et al. (2016) showed slight waveform differences with a bifurcation at OP2 occurring at a younger age than would typically be expected. A further waveform characterization of the OP traces will enable us to determine the contribution of the amacrine cells to the primary measure of b-wave amplitude. The OP contribution may indicate further downstream changes in the retina associated with amacrine cell inhibitory circuits to the ON pathway (Wachtmeister 1998).

A further consideration is the reduced a-wave amplitude that is mainly produced by closing cGMP gated ion channels in the outer segment that reduces glutamate release. Thus a reduction in hyperpolarization as indicated by the reduced a-wave amplitude, would result in more glutamate in the post receptoral space and an activation of the G-protein coupled mGLUR6 receptor and an increase in G_{α} closing of the transient receptor potential cation channel subfamily M member 1 (TRMP1) cation channels in the ON-bipolar cells thus reducing their depolarization (Shen et al. 2012). This would be the equivalent ERG to a weaker flash. The reduced a-wave may reflect a lower sensitivity to the retina to light, as evidenced by the reduced DA b-waves previously reported (Constable et al. 2016; Ritvo et al. 1988), in which the main rod bipolar cell depolarization is driven by rod hyperpolarization in this simpler synapse between multiple rod photoreceptors and a single rod bipolar and horizontal cell. Importantly in mouse models of ASD a reduced a-wave under DA conditions has been reported (Guimaraes-Souza et al. 2019) and reduced rhodopsin levels have been found in mice models of Fragile X- syndrome (Rossignol et al. 2014) that may also contribute to retinal sensitivity under DA conditions.

Another factor to consider is the development of the delicate ribbon synapses that form between the cone pedicles with the triad of bipolar and horizontal cells. These ensure the correct localization of synaptic vesicles in the cone adjacent to receptors in the horizontal and bipolar cells (Mercer and Thoreson 2011). If this structural order was impaired in ASD then synaptic transmission would be compromised. In addition, transport carriers and regulation of the key neurotransmitters for bipolar cells (glutamate) and horizontal cells (GABA) may also be dysfunctional in the retina and contribute to the imbalance in response associated with the b-wave amplitude (Bush and Sieving 1994; Eggers and Lukasiewicz 2006; Hanna and Calkins 2007; Dhingra and Vardi 2012).

Not surprisingly, given the heterogeneity of ASD, with many gene clusters and environmental factors contributing to an individual's phenotype, the ability of the ERG b-wave to discriminate ASD from the

control group was moderate, with an AUC of approximately 0.7 and no significant correlations with broad ASD phenotype scores of ADOS and autism severity.

There are several limitations of the study to be addressed in future research. Despite statistically controlling for factors of sex, ethnicity and iris color, unmeasured differences may have affected results. For sex, there are reports that the ERG amplitude in adults is slightly higher in females compared to males (Birch and Anderson 1992; Zeidler 1959; Kato et al. 2017), although it is unclear whether this difference is also present in children. The sex balance in the groups, with a 3:1 bias of males in the ASD group is representative of this population (Baird et al. 2006; Bertrand et al. 2001). The higher prevalence of Caucasian subjects in the ASD compared to the control group may also be a source of uncertainty for the results with different genetic backgrounds that cannot be fully accounted for. The darker iris colors in the control group are a presumed indicator of choroidal pigmentation and may not truly reflect the amount of melanin in the retinal pigment epithelium and underlying melanocytes in the choroid where the light is absorbed. It is known that ERG amplitudes are higher in individuals with lighter fundi (Wali and Leguire 1992), and iris pigmentation is associated with lower b-wave amplitudes for the LA ERG at flash strengths near the peak of the photopic hill but not at the higher saturating strengths associated with the ON- pathway (Al Abdlseaed et al. 2010). The assumption is that the iris color index gives a correlated value to the degree of pigmentation on the fundus and hence the amount of light that could be absorbed by melanin and not the photoreceptor opsins. It may be that skin pigmentation could be a better index and would require further studies to quantify the correlation between the iris color index and choroidal pigmentation. We also did not correct for repeated measures as this study's aim was to explore the differences in the ERG waveform in ASD and provide a clinically significant diagnostic biomarker.

In addition, the pupils were not dilated in this study to reduce the associated stress with blurred vision and photophobia after mydriasis. As noted, the lower background luminance may affect the peak value

of the photopic hill (Gagné et al. 2010). However, since the adoption of the RETeval as a device for clinical recordings, several studies have compared the results of the RETeval to conventional dilated ERG measurements. There is a good correlation with the dilated ERG to the undilated ERGs recoded with the RETeval (Liu et al. 2018). In addition, the clinical use of the undilated protocol has also been demonstrated in a small study in children under three years of age taking vigabatrin when compared to standard dilated ERGs (Ji et al. 2019). Flicker ERGs amplitudes are also reported to be non-significantly different ($p > .31$) and implicit times ($p > .86$) when recorded with the RETeval under dilated or undilated conditions in patients with cataracts. Whilst, we acknowledge that dilation is advantageous for recording the ERG, there is good support for the undilated protocol utilized by the RETeval device.

In order to address the heterogeneity inherent within the study population a subsequent analysis in a homogeneous subset consisting of only Caucasian males in which there was no comorbidity or use of CNS medications and no sibling in the family with ASD yielded a stronger group difference despite reducing the sample size with the most statistically significant finding occurring at the highest flash strength of log 1.2 phot cd.s.m^{-2} ($p<0.001$, $z= 4.21$). This result suggests that the ERG may be limited in being able to find strong group differences only in relatively homogeneous populations which is not characteristic of ASD. Furthermore, this result may help explain one further limitation in the study design, where only two of the three centers contributed comparison/control subjects, and one center contributed only ASD participants. At the highest flash strength at one centre there was no significant difference ($p=.24$) whilst at the other center there was a group difference in b-wave amplitude ($p=.003$). The disparity between the two centers may be driven by a larger heterogeneity in one of the centers compared to the other. One factor is the ethnic background of participants that once adjusted for in the Caucasian only group resulted in significant findings within these centers at .398 log phot cd.s.m^{-2} ($p <.05$) and an overall larger difference in b-wave amplitudes at the strongest flash strength. given that when heterogeneity is reduced the group difference is greater across the centers.

One final limitation was that we were unable to extend the flash strength beyond 1.2 log phot cd.s.m^{-2} because we did not dilate the pupils and this was the maximal flash strength obtainable using the Troland protocol. It would have been advantageous to extend the photopic hill a further log unit to ascertain if at even stronger flash strengths the group differences were greater.

A next step in this line of research would be to look at younger children who may be at risk of developing ASD due to a sibling within the family with the diagnosis as has been demonstrated in other studies into schizophrenia and bipolar disorder (Gagné et al. 2019, Hébert et al. 2010) Given the strongest differences between groups were evident only when a gender, age and ethnically matched sub-set were used it may be that the ERG is unable to discriminate effectively and the strong familial associations evident in schizophrenia and bipolar disorder may not be present in families with ASD children. Therefore, additional, studies investigating these findings in relation to other conditions, such as ADHD and OCD, may help to determine if these findings relate specifically to ASD or are simply a marker for atypical neurodevelopment within the CNS. Furthermore, the diagnostic capability of a test to distinguish an individual group may be limited owing to the overlapping nature neurodevelopmental disorders (Baribeau et al. 2019; Dajani et al. 2019; Taylor et al. 2019; Lavoie et al. 2014). We note that our sample, school-aged and older, is also poorly suited to examine diagnostic utility and future studies should examine the ERG in earlier childhood. Nonetheless the LA-ERG waveform is atypical in ASD, a neurodevelopmental condition which differs from neurodevelopmental and neurodegenerative conditions in which the ERG waveform also has been found to be altered, such as schizophrenia, bipolar disorder (Hébert et al. 2015; Hébert et al. 2020) and Parkinson's disease (Nowacka et al. 2015).

It is of interest to consider the findings of this study with those in schizophrenia (Hébert et al. 2015; Hébert et al. 2020), given both conditions share similarities with poor communication and social interaction as well as cognitive function such as theory of mind (Chung et al. 2014, Chisholm et al. 2015). In addition, there are genetic overlaps between schizophrenia and ASD that contribute to

synaptic formation (Kenny et al. 2014, Pathania et al. 2015, Luo et al. 2018) and glutamate signaling (Habela et al. 2015). The extensive work by Hébert's groups work into identifying differences in the ERG waveform in individuals with schizophrenia (Hébert et al. 2015; Hébert et al. 2020), and those at risk (Hébert et al. 2010) finds some similarities with the present study in these linked conditions (Chisholm et al. 2015). In schizophrenia, for example, a similar pattern of results has been reported with a reduced a- and b-wave amplitude and delayed b-wave peak in schizophrenia which we also observed in the ASD cohort. However, the effect sizes at V_{max} (4 cd.s.m^{-2}) are lower in this study compared to those reported in schizophrenia where for the b-wave amplitude in ASD the univariable effect size is -.28 compared to -.49 in schizophrenia, and the b- wave time effect size is .24 in ASD compared to 1.29 in schizophrenia and the a-wave amplitude's effect size in ASD is -.27 compared to -.70 in schizophrenia. Thus, there is a greater effect on the ERG waveform in schizophrenia compared to ASD. These differences may be related to the continuum of neurodevelopmental conditions from depression/anxiety to ASD, bipolar and schizophrenia or simply that the ASD phenotype is more heterogeneous than schizophrenia with greater genetic variation and therefore the ERG effects are smaller in this group.

The ERG may provide a wider clinical utility as a factor not just for children with ASD, but others who may be at risk of atypical neurodevelopment.

Conclusions

This large, multicenter study of children shows the LA-ERG is a potential marker for neurodevelopmental conditions such as ASD in children. By providing a reproducible, non-invasive and robust measure of CNS activity the ERG can help our understanding of the impact of genetic interaction and complexity in ASD and aid drug discovery that targets CNS development of signaling pathways common to the CNS and retina.

Acknowledgements

The authors would like to thank the participants and their families for their support. Quentin Davis and Joshua Santosa of LKC Technologies for programming the RETeval custom protocol.

References

Al Abdlseaed, A., McTaggart, Y., Ramage, T., Hamilton, R., & McCulloch, D. L. (2010). Light- and dark-adapted electroretinograms (ERGs) and ocular pigmentation: comparison of brown- and blue-eyed cohorts. *Doc Ophthalmol*, 121(2), 135-146.

An, J. Y., Lin, K., Zhu, L., Werling, D. M., Dong, S., Brand, H., et al. (2018). Genome-wide de novo risk score implicates promoter variation in autism spectrum disorder. *Science*, 362(6420), doi:10.1126/science.aat6576.

APA. (2013). *Diagnostic and statistical manual of mental disorders (5th ed.). Arlington, VA: American Psychiatric Publishing.* Arlington, VA: : American Psychiatric Publishing.

Autism Genome Project, (2007). Mapping autism risk loci using genetic linkage and chromosomal rearrangements. *Nat Genet*, 39(3), 319-328.

Baird, G., Simonoff, E., Pickles, A., Chandler, S., Loucas, T., Meldrum, D., et al. (2006). Prevalence of disorders of the autism spectrum in a population cohort of children in South Thames: the Special Needs and Autism Project (SNAP). *The Lancet*, 368(9531), 210-215.

Baribeau, D. A., Dupuis, A., Paton, T. A., Hammill, C., Scherer, S. W., Schachar, R. J., et al. (2019). Structural neuroimaging correlates of social deficits are similar in autism spectrum disorder and attention-deficit/hyperactivity disorder: analysis from the POND Network. *Transl Psychiatry*, 9(1), 72. doi:10.1038/s41398-019-0382-0.

Bertrand, J., Mars, A., Boyle, C., Bove, F., Yeargin-Allsopp, M., & Decoufle, P. (2001). Prevalence of Autism in a United States Population: The Brick Township, New Jersey, Investigation. *Pediatrics,* 108(5), 1155-1161.

Birch, D. G., & Anderson, J. L. (1992). Standardized Full-Field Electroretinography: Normal values and their variation with age. *JAMA Ophthalmology*, 110(11), 1571-1576.

Bush, R. A., & Sieving, P. A. (1994). A proximal retinal component in the primate photopic ERG a-wave. *Invest Ophthalmol Vis Sci,* 35(2), 635-645.

Chapot, C. A., Euler, T., & Schubert, T. (2017). How do horizontal cells 'talk' to cone photoreceptors? Different levels of complexity at the cone-horizontal cell synapse. *J Physiol,* 595(16), 5495-5506.

Chaste, P., & Leboyer, M. (2012). Autism risk factors: genes, environment, and gene-environment interactions. *Dialogues Clin Neurosci,* 14(3), 281-292.

Chisholm, K., Lin, A., Abu-Akel, A., & Wood, S. J. (2015). The association between autism and schizophrenia spectrum disorders: A review of eight alternate models of co-occurrence. *Neurosci Biobehav Rev,* 55, 173-183.

Chung, Y.S., Barch, D., Strube, M., 2014. A meta-analysis of mentalizing impairments in adults with schizophrenia and autism spectrum disorder. *Schizophr. Bull*. 40(3), 602–616.

Coghlan, S., Horder, J., Inkster, B., Mendez, M. A., Murphy, D. G., & Nutt, D. J. (2012). GABA system dysfunction in autism and related disorders: from synapse to symptoms. *Neurosci Biobehav Rev,* 36(9), 2044-2055.

Constable, P. A., Gaigg, S. B., Bowler, D. M., Jägle, H., & Thompson, D. A. (2016). Full-field electroretinogram in autism spectrum disorder. *Doc Ophthalmol,* 132(2), 83-99

Dai, H., Jackson, C. R., Davis, G. L., Blakely, R. D., & McMahon, D. G. (2017). Is dopamine transporter-mediated dopaminergic signaling in the retina a noninvasive biomarker for attention-deficit/ hyperactivity disorder? A study in a novel dopamine transporter variant Val559 transgenic mouse model. *J Neurodev Disord,* 9(1), 38.

Dajani, D. R., Burrows, C. A., Odriozola, P., Baez, A., Nebel, M. B., Mostofsky, S. H., et al. (2019). Investigating functional brain network integrity using a traditional and novel categorical scheme for neurodevelopmental disorders. *Neuroimage Clin,* 21, 101678. doi:10.1016/j.nicl.2019.101678.

Dhingra, A., & Vardi, N. (2012). mGlu receptors in the retina. *Wiley Interdisciplinary Reviews: Membrane Transport and Signaling*, 1(5), 641-653.

Doherty, J., Cooper, M., & Thapar, A. (2018). Advances in our understanding of the genetics of childhood neurodevelopmental disorders. *Evid Based Ment Health,* 21(4), 171-172.

Eggers, E. D., & Lukasiewicz, P. D. (2006). Receptor and transmitter release properties set the time course of retinal inhibition. *J Neurosci,* 26(37), 9413-9425.

Fatemi, S. H., & Folsom, T. D. (2015). GABA receptor subunit distribution and FMRP-mGluR5 signaling abnormalities in the cerebellum of subjects with schizophrenia, mood disorders, and autism. *Schizophr Res*, 167(1-3), 42-56.

Gadow, K. D., Roohi, J., DeVincent, C. J., Kirsch, S., & Hatchwell, E. (2010). Glutamate transporter gene (SLC1A1) single nucleotide polymorphism (rs301430) and repetitive behaviors and anxiety in children with autism spectrum disorder. *J Autism Dev Disord*, 40(9), 1139-1145.

Gagné, A. M., Moreau, I., St-Amour, I., Marquet, P., & Maziade, M. (2019). Retinal function anomalies in young offspring at genetic risk of schizophrenia and mood disorder: The meaning for the illness pathophysiology. Schizophr Res.

Gagné, A. M., Lavoie, J., Lavoie, M. P., Sasseville, A., Charron, M. C., & Hébert, M. (2010). Assessing the impact of non-dilating the eye on full-field electroretinogram and standard flash response. *Doc Ophthalmol*, 121(3), 167-175.

Gotham, K., Pickles, A., & Lord, C. (2009). Standardizing ADOS scores for a measure of severity in autism spectrum disorders. *J Autism Dev Disord*, 39(5), 693-705.

Grove, J., Ripke, S., Als, T. D., Mattheisen, M., Walters, R. K., Won, H., et al. (2019). Identification of common genetic risk variants for autism spectrum disorder. *Nat Genet*, 51(3), 431-444.

Guimaraes-Souza, E. M., Joselevitch, C., Britto, L. R. G., & Chiavegatto, S. (2019). Retinal alterations in a pre-clinical model of an autism spectrum disorder. *Mol Autism,* 10, 19, doi:10.1186/s13229-019-0270-8.

Habela, C. W., Song, H., & Ming, G. L. (2015). Modeling synaptogenesis in schizophrenia and autism using human iPSC derived neurons. *Mol Cell Neurosci*, doi:10.1016/j.mcn.2015.12.002.

Hadley, D., Wu, Z. L., Kao, C., Kini, A., Mohamed-Hadley, A., Thomas, K., et al. (2014). The impact of the metabotropic glutamate receptor and other gene family interaction networks on autism. *Nat Commun,* 5, 4074, doi:10.1038/ncomms5074.

Hamilton, R., Bees, M. A., Chaplin, C. A., & McCulloch, D. L. (2007). The luminance-response function of the human photopic electroretinogram: a mathematical model. *Vision Res,* 47(23), 2968-2972.

Hanna, M. C., & Calkins, D. J. (2007). Expression of genes encoding glutamate receptors and transporters in rod and cone bipolar cells of the primate retina determined by single-cell polymerase chain reaction. *Mol Vis,* 13, 2194-2208.

Hébert, M., Gagné, A. M., Paradis, M. E., Jomphe, V., Roy, M. A., Mérette, C., et al. (2010). Retinal response to light in young nonaffected offspring at high genetic risk of neuropsychiatric brain disorders. Biol Psychiatry, 67(3), 270-274.

Hébert, M., Merette, C., Gagne, A. M., Paccalet, T., Moreau, I., Lavoie, J., et al. (2020). The electroretinogram may differentiate schizophrenia from bipolar disorder. *Biol Psychiatry, 3*(1), 263-270.

Hébert, M., Merette, C., Paccalet, T., Emond, C., Gagne, A. M., Sasseville, A., et al. (2015). Light evoked potentials measured by electroretinogram may tap into the neurodevelopmental roots of schizophrenia. *Schizophr Res, 162*(1-3), 294-295.

Hébert, M., Merette, C., Paccalet, T., Gagne, A. M., & Maziade, M. (2017). Electroretinographic anomalies in medicated and drug free patients with major depression: Tagging the developmental roots of major psychiatric disorders. *Prog Neuropsychopharmacol Biol Psychiatry*, 75, 10-15.

Hobby, A. E., Kozareva, D., Yonova-Doing, E., Hossain, I. T., Katta, M., Huntjens, B., et al. (2018). Effect of varying skin surface electrode position on electroretinogram responses recorded using a handheld stimulating and recording system. *Doc Ophthalmol*, 137(2), 79-86.

Hoerder-Suabedissen, A., Oeschger, F. M., Krishnan, M. L., Belgard, T. G., Wang, W. Z., Lee, S., et al. (2013). Expression profiling of mouse subplate reveals a dynamic gene network and disease association with autism and schizophrenia. *Proc Natl Acad Sci USA*, 110(9).

Holopigian, K., Clewner, L., Seiple, W., Kupersmith, M.J. (1994). The effects of dopamine blockade on the human flash electroretinogram. *Doc Ophthalmol*, 86:1-10.

Ji, X., McFarlane, M., Liu, H., Dupuis, A., & Westall, C. A. (2019). Hand-held, dilation-free, electroretinography in children under 3 years of age treated with vigabatrin. *Doc Ophthalmol*, 138(3), 195-203.

Kato, K., Kondo, M., Nagashima, R., Sugawara, A., Sugimoto, M., Matsubara, H., et al. (2017). Factors affecting mydriasis-free flicker ERGs recorded with real-time correction for retinal illuminance: Study of 150 young healthy subjects. *Invest Ophthalmol Vis Sci, 58*(12), 5280-5286.

Kenny, E. M., Cormican, P., Furlong, S., Heron, E., Kenny, G., Fahey, C., et al. (2014). Excess of rare novel loss-of-function variants in synaptic genes in schizophrenia and autism spectrum disorders. *Mol Psychiatry*, 19(8), 872-879.

Lachapelle, P., Rufiange, M., & Dembinska, O. (2001). A physiological basis for definition of the ISCEV ERG standard flash (SF) based on the photopic hill. *Doc Ophthalmol*, 102(2), 157-162.

Lavoie, J., Illiano, P., Sotnikova, T. D., Gainetdinov, R. R., Beaulieu, J.-M., & Hébert, M. (2014). The Electroretinogram as a Biomarker of Central Dopamine and Serotonin: Potential Relevance to Psychiatric Disorders. *Biol Psychiatry*, 75(6), 479-486.

Lavoie, J., Maziade, M., & Hebert, M. (2014). The brain through the retina: the flash electroretinogram as a tool to investigate psychiatric disorders. *Prog Neuropsychopharmacol Biol Psychiatry*, 48, 129-134.

Liu, H., Ji, X., Dhaliwal, S., Rahman, S. N., McFarlane, M., Tumber, A., et al. (2018). Evaluation of light- and dark-adapted ERGs using a mydriasis-free, portable system: clinical classifications and normative data. *Doc Ophthalmol*, 137(3), 169-181.

Luo, J., Norris, R. H., Gordon, S. L., & Nithianantharajah, J. (2018). Neurodevelopmental synaptopathies: Insights from behaviour in rodent models of synapse gene mutations. *Prog Neuropsychopharmacol Biol Psychiatry*, 84(Pt B), 424-439.

Luyster, R., Gotham, K., Guthrie, W., Coffing, M., Petrak, R., Pierce, K., et al. (2009). The Autism Diagnostic Observation Schedule-toddler module: a new module of a standardized diagnostic measure for autism spectrum disorders. *J Autism Dev Disord,* 39(9), 1305-1320.

McCulloch, D. L., Kondo, M., Hamilton, R., Lachapelle, P., Messias, A. M. V., Robson, A. G., et al. (2019). ISCEV extended protocol for the stimulus-response series for light-adapted full-field ERG. *Doc Ophthalmol,* 138(3), 205-215.

McCulloch, D. L., Marmor, M. F., Brigell, M. G., Hamilton, R., Holder, G. E., Tzekov, R., et al. (2015). ISCEV Standard for full-field clinical electroretinography (2015 update). *Doc Ophthalmol,* 130(1), 1-12.

McPartland, J. C. (2016). Considerations in biomarker development for neurodevelopmental disorders. *Curr Opin Neurol,* 29(2), 118-122.

Mercer, A. J., & Thoreson, W. B. (2011). The dynamic architecture of photoreceptor ribbon synapses: cytoskeletal, extracellular matrix, and intramembrane proteins. *Vis Neurosci*, 28(6), 453-471.

Miura, G., Baba, T., Oshitari, T., & Yamamoto, S. (2018). Flicker electroretinograms of eyes with cataract recorded with RETeval system before and after mydriasis. *Clin Ophthalmol*, 12, 427-432.

Nowacka, B., Lubinski, W., Honczarenko, K., Potemkowski, A., & Safranow, K. (2015). Bioelectrical function and structural assessment of the retina in patients with early stages of Parkinson's disease (PD). *Doc Ophthalmol*, 131(2), 95-104.

Pathania, M., Davenport, E. C., Muir, J., Sheehan, D. F., Lopez-Domenech, G., & Kittler, J. T. (2014). The autism and schizophrenia associated gene CYFIP1 is critical for the maintenance of dendritic complexity and the stabilization of mature spines. *Transl Psychiatry, 4*, e374, doi:10.1038/tp.2014.16.

Pizzarelli, R., & Cherubini, E. (2011). Alterations of GABAergic signaling in autism spectrum disorders. *Neural Plast*, 2011, 297153, doi:10.1155/2011/297153.

Popova, E. (2014). Role of dopamine in distal retina. *J Comp Physiol*, 200(5), 333-358.

Popova, E., & Kupenova, P. (2017). Interaction between the serotoninergic and GABAergic systems in frog retina as revealed by electroretinogram. *Acta Neurobiol Exp*, 77(4), 351-361.

Realmuto, G., Purple, R., Knobloch, W., & Ritvo, E. (1989). Electroretinograms (ERGs) in four autistic probands and six first-degree relatives. *Can J Psychiatry*, 34(5), 435-439.

Ritvo, E. R., Creel, D., Realmuto, G., Crandall, A. S., Freeman, B. J., Bateman, J. B., et al. (1988). Electroretinograms in autism: a pilot study of b-wave amplitudes. *Am J Psychiatry,* 145(2), 229-232.

Robson, A. G., Nilsson, J., Li, S., Jalali, S., Fulton, A. B., Tormene, A. P., et al. (2018). ISCEV guide to visual electrodiagnostic procedures. *Doc Ophthalmol, 136*(1), 1-26.

.

Rossignol, R., Ranchon-Cole, I., Paris, A., Herzine, A., Perche, A., Laurenceau, D., et al. (2014). Visual sensorial impairments in neurodevelopmental disorders: evidence for a retinal phenotype in Fragile X Syndrome. *PLoS One, 9*(8), e105996,

Sanders, S. J., He, X., Willsey, A. J., Ercan-Sencicek, A. G., Samocha, K. E., Cicek, A. E., et al. (2015). Insights into autism spectrum disorder genomic architecture and biology from 71 Risk Loci. *Neuron,* 87(6), 1215-1233.

Schwitzer, T., Lavoie, J., Giersch, A., Schwan, R., & Laprevote, V. (2015). The emerging field of retinal electrophysiological measurements in psychiatric research: A review of the findings and the perspectives in major depressive disorder. *J Psychiatr Res,* 70, 113-120.

Shen,Y., Rampino, M.A., Carroll, R.C., Nawy, S. (2012) G-protein-mediated inhibition of the Trp channel TRPM1 requires the $G_{\beta\gamma}$ dimer. *PNAS,* 109:8752-8757.

Taylor, M. J., Martin, J., Lu, Y., Brikell, I., Lundstrom, S., Larsson, H., et al. (2019). Association of genetic risk factors for psychiatric disorders and traits of these disorders in a Swedish population twin sample. *JAMA Psychiatry,* 76(3), 280-289.

Thoreson, W.B & Mangel, S.C. (2012).Lateral interactions in the outer retina. *Prog Ret Res,* 31:407-441.

Ueno, S., Kondo, M., Niwa, Y., Terasaki, H., & Miyake, Y. (2004). Luminance dependence of neural components that underlies the primate photopic electroretinogram. *Invest Ophthalmol Vis Sci,* 45(3), 1033-1040.

Uzunova, G., Hollander, E., & Shepherd, J. (2014). The role of ionotropic glutamate receptors in childhood neurodevelopmental disorders: autism spectrum disorders and fragile x syndrome. *Curr Neuropharmacol,* 12(1), 71-98.

Wachtmeister, L. (1998). Oscillatory potentials in the retina: what do they reveal. *Prog Retin Eye Res,* 17(4), 485-521.

Wali, N., & Leguire, L. E. (1992). Fundus pigmentation and the dark-adapted electroretinogram. *Doc Ophthalmol,* 80(1), 1-11.

Wechsler, D. (1999). *Wechsler Abbreviated Intelligence Scale* San Antonio, TX: The Psychological Corporation.

Wechsler, D. (2003). *Wechsler Intelligence Scale for Children-Fourth Edition* San Antonio, TX: The Psychological Corporation.

Youssef, P., Nath, S., Chaimowitz, G. A., & Prat, S. S. (2019). Electroretinography in psychiatry: A systematic literature review. *European Psychiatry,* 62, 97-106.

Yu, L., Wu, Y., & Wu, B. L. (2015). Genetic architecture, epigenetic influence and environment exposure in the pathogenesis of Autism. *Sci China Life Sci,* 58(10), 958-967.

Zhang, X., Piano, I., Messina, A., D'Antongiovanni, V., Cro, F., Provenzano, G., et al. (2019). Retinal defects in mice lacking the autism-associated gene Engrailed-2. *Neuroscience*, doi:10.1016/j.neuroscience.2019.03.061.

TABLE OF CONTENTS

CNS MEDICATIONS AND HOMOGENEITY

CNS medications

When b-wave amplitude was reanalyzed between groups excluding those taking a CNS acting medication there was no overall change in the findings with the main significant difference between groups occurring at log 1.2 cd.s.m^{-2} (p=.003), z=3.02. The ASD group consisted of n=141 eyes aged 12.9 (4.4) years old and the control group contained n=171 eyes aged 13.8 (4.8) years old.

Flash strength log phot cd.s.m^{-2}	No CNS medications b-wave amplitudes, mean (SEM)		
	ASD	Control	p, (z-score)
-.367	10.7 (1.4)	12.4 (1.5)	.10, (1.63)
-.119	15.7 (1.4)	17.1 (1.4)	.16, (1.40)
.114	23.6 (1.4)	25.8 (1.4)	.022*, (2.28)
.398	30.6 (1.4)	33.2 (1.4)	.006**, (2.73)
.602	31.9 (1.4)	34.1 (1.4)	.021*, (2.30)
.799	30.4 (1.4)	31.9 (1.4)	.12, (1.57)
.949	28.4 (1.4)	29.6 (1.4)	.20, (1.29)
1.114	26.7 (1.4)	28.6 (1.4)	.042*, (2.04)
1.204	26.7 (1.4)	29.7 (1.4)	.003**, (3.02)

Table 1 of b-wave amplitude in participants not taking any medications targeting the CNS.

Homogeneous Analysis

When a subset of the study population was analyzed including n=41 eyes from the control and n= 63 eyes from the ASD population where all subjects were male, Caucasian, under 16 years of age and not taking any medications acting on the CNS then the most significant group difference for the b-wave amplitude was at log 1.2 phot cd.s.m^{-2} (p<.001, z=4.21). The sample included n=61 eyes in the ASD group and n=41 eyes in the control group aged 11.6 (2.4) and 11.9 (2.8) years respectfully.

Flash strength log phot cd.s.m^{-2}	Homogeneous Analysis b-wave amplitudes, mean (SEM)		
	ASD	Control	p, (z-score)
-.367	11.0 (1.8)	13.9 (2.1)	.08, (1.74)
-.119	15.8 (1.8)	18.9 (2.0)	.05, (1.93)
.114	23.3 (1.8)	27.8 (2.0)	.004**, (2.88)
.398	30.1 (1.8)	35.6 (2.0)	<.001***, (3.48)
.602	31.4 (1.8)	36.6 (2.0)	.001***, (3.40)
.799	29.9 (1.8)	34.6 (2.0)	.002**, (3.04)
.949	27.8 (1.8)	32.4 (2.0)	.003**, (2.92)
1.114	25.8 (1.8)	31.4 (2.0)	<.001***, (3.60)
1.204	25.5 (1.8)	32.5 (2.0)	<.001**, (4.21)

Table 2 of b-wave amplitudes for a sub-set of participants who were all male, less than 16 years of age, not taking CNS medications and were all Caucasian. The ASD group had a sole diagnosis of ASD without a co-morbidity.

Percentage of Included Traces

Flash Strength Log phot cd.s.m^{-2}	**ASD (%) a-wave**	**Control (%) a-wave**	**ASD (%) b-wave**	**Control (%) b-wave**
-0.367	90.3 (160)	97.7 (170)	91.5 (162)	100.0 (174)
-0.119	94.4 (167)	96.6 (168)	96.0 (170)	96.6 (171)
0.114	95.5 (169)	98.3 (171)	96.6 (171)	98.9 (172)
0.398	97.2 (172)	98.9 (172)	98.9 (175)	98.9 (172)
0.602	97.2 (172)	97.1 (169)	97.7 (173)	98.3 (171)
0.799	97.7 (173)	99.4 (173)	97.7 (173)	99.4 (173)
0.949	96.0 (170)	98.3 (171)	96.6 (171)	98.9 (172)
1.114	96.0 (170	99.4 (173)	97.2 (172)	99.4 (173)
1.204	96.6 (171)	100.0 (174)	97.2 (172)	100.0 (174)
0.477 ISCEV Standard	89.2 (157)	93.6 (163)	90.3 (160)	93.8 (163)

The percentage and number (in brackets) of included measures of the a- and b-wave for the ASD and TD groups for each of the 10 flash strengths in the study.

Sample Report

Patient Information

Patient ID: GA023
Birthdate: July 18, 2008
Test started: December 18, 2018, 4:31 PM
Report generated: December 18, 2018, 5:21 PM

Device Information

RET*eval*™
Manufacturer: LKC Technologies, Inc.
Serial number: R001053
Firmware version: 2.9.4 Reference data: 2018.21 9a54517
Test protocol: ASD Custom Protocol - Photopic Flash Series - Td
Electrodes: Sensor Strips

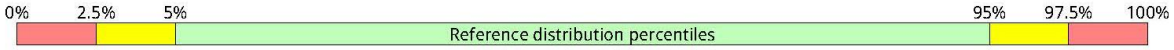

Test #1: Flash: 71 Td·s, Chromaticity (0.33, 0.33) at 2 Hz Background: 1100 Td, Chromaticity (0.33, 0.33)

Right Eye (Pupil 3.1 mm)

	a-wave		b-wave	
	ms	µV	ms	µV
1	12.8	-11.9	26.1	50.4
2	13.0	-14.1	26.0	45.0
	12.9	-13.0	26.1	47.7

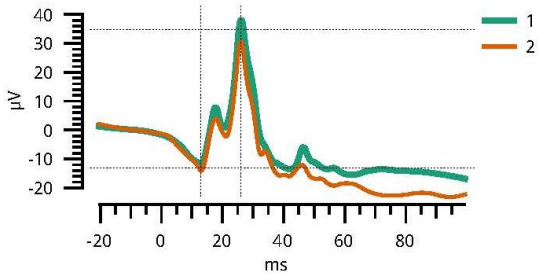

Left Eye (Pupil 2.6 mm)

	a-wave		b-wave	
	ms	µV	ms	µV
1	11.7	-5.3	25.8	33.4
2	12.7	-7.4	25.8	39.8
	12.2	-6.3	25.8	36.6

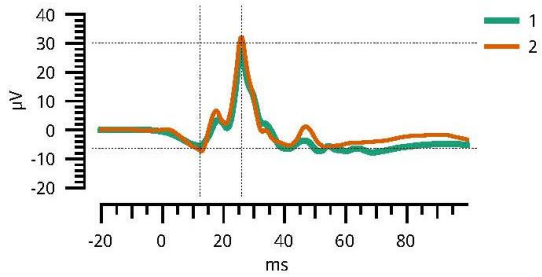

Test #2: Flash: 110 Td·s, Chromaticity (0.33, 0.33) at 2 Hz Background: 1100 Td, Chromaticity (0.33, 0.33)

Right Eye (Pupil 3.0 mm)

	a-wave		b-wave	
	ms	µV	ms	µV
1	10.3	-12.5	27.7	38.5
2	10.1	-8.3	27.1	41.4
	10.2	-10.4	27.4	40.0

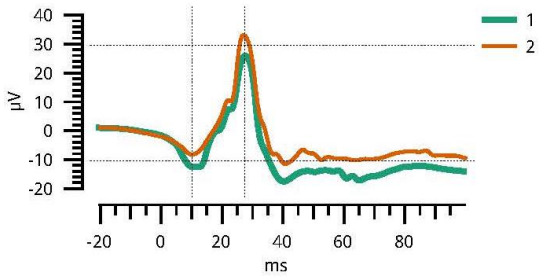

Left Eye (Pupil 2.5 mm)

	a-wave		b-wave	
	ms	µV	ms	µV
1	10.8	-9.2	27.8	44.6
2	10.2	-8.8	27.4	39.6
	10.5	-9.0	27.6	42.1

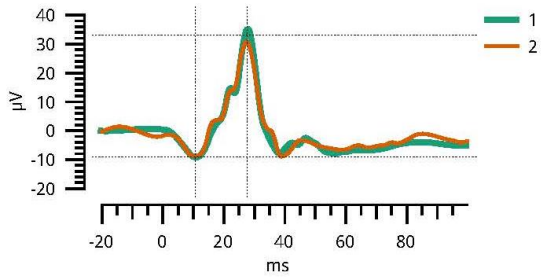

Patient ID: GA023
Birthdate: July 18, 2008
Test started: December 18, 2018, 4:31 PM
Report generated: December 18, 2018, 5:21 PM

Test #3: Flash: 36 Td·s, Chromaticity (0.33, 0.33) at 2 Hz Background: 1100 Td, Chromaticity (0.33, 0.33)

Right Eye (Pupil 2.9 mm)

	a-wave		b-wave	
	ms	µV	ms	µV
1	12.5	-7.2	24.2	40.2
2	13.1	-9.9	24.1	45.5
	12.8	-8.6	24.2	42.8

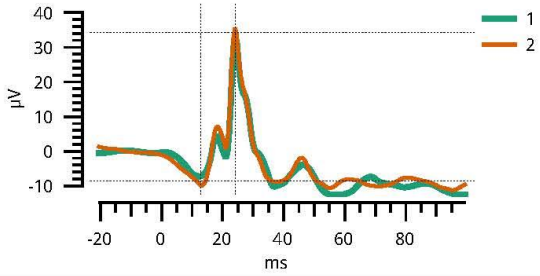

Left Eye (Pupil 2.5 mm)

	a-wave		b-wave	
	ms	µV	ms	µV
1	12.9	-7.1	24.2	31.3
2	12.5	-6.9	24.0	42.0
	12.7	-7.0	24.1	36.6

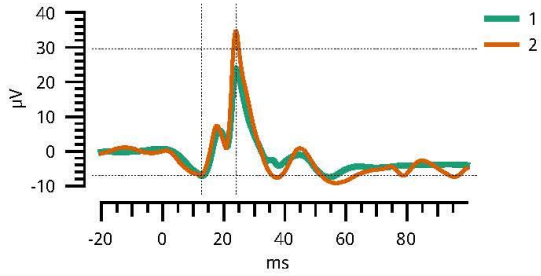

Test #4: Flash: 250 Td·s, Chromaticity (0.33, 0.33) at 2 Hz Background: 1100 Td, Chromaticity (0.33, 0.33)

Right Eye (Pupil 2.2 mm)

	a-wave		b-wave	
	ms	µV	ms	µV
1	11.3	-14.6	28.8	44.5
2	10.8	-11.0	28.8	34.1
	11.1	-12.8	28.8	39.3

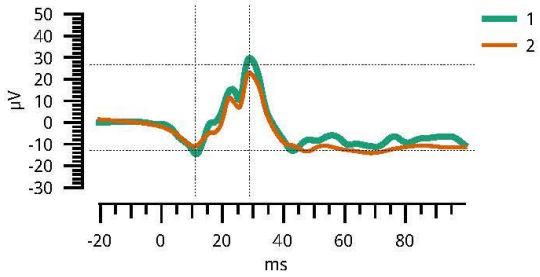

Left Eye (Pupil 2.4 mm)

	a-wave		b-wave	
	ms	µV	ms	µV
1	10.1	-10.5	28.7	41.1
2	11.1	-13.9	29.3	37.5
	10.6	-12.2	29.0	39.3

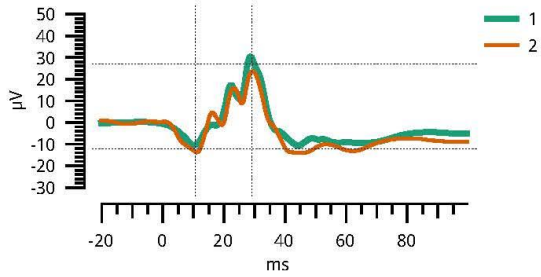

Patient ID: GA023
Birthdate: July 18, 2008
Test started: December 18, 2018, 4:31 PM
Report generated: December 18, 2018, 5:21 PM

Test #5: Flash: 180 Td·s, Chromaticity (0.33, 0.33) at 2 Hz Background: 1100 Td, Chromaticity (0.33, 0.33)

Right Eye (Pupil 2.2 mm)

	a-wave		b-wave	
	ms	µV	ms	µV
1	10.9	-9.7	28.1	41.9
2	10.9	-8.3	28.4	36.7
	10.9	-9.0	28.3	39.3

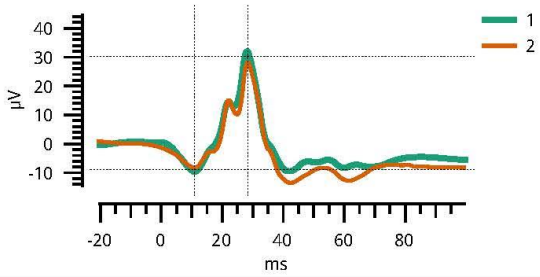

Left Eye (Pupil 2.9 mm)

	a-wave		b-wave	
	ms	µV	ms	µV
1	11.1	-8.7	28.3	41.9
2	11.8	-6.7	28.8	31.5
	11.5	-7.7	28.6	36.7

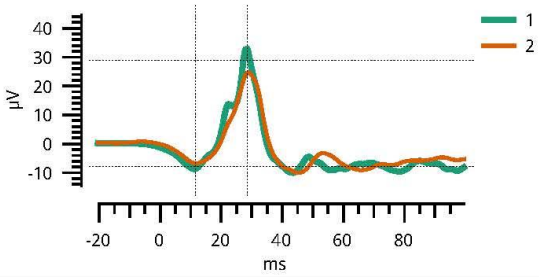

Test #6: Flash: 450 Td·s, Chromaticity (0.33, 0.33) at 2 Hz Background: 1100 Td, Chromaticity (0.33, 0.33)

Right Eye (Pupil 2.4 mm)

	a-wave		b-wave	
	ms	µV	ms	µV
1	11.0	-13.1	30.1	38.7
2	11.1	-10.2	30.2	37.7
	11.0	-11.7	30.1	38.2

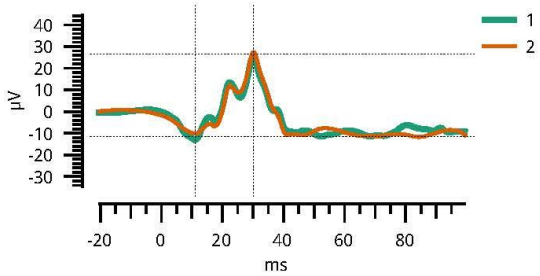

Left Eye (Pupil 2.5 mm)

	a-wave		b-wave	
	ms	µV	ms	µV
1	12.3	-8.3	30.4	34.1
2	11.4	-16.2	30.2	42.7
3	11.2	-12.0	30.1	35.7
	11.6	-12.2	30.2	37.5

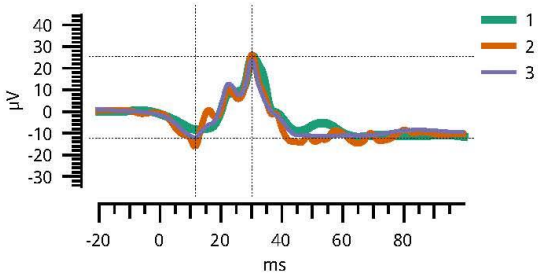

Patient ID: GA023
Birthdate: July 18, 2008
Test started: December 18, 2018, 4:31 PM
Report generated: December 18, 2018, 5:21 PM

Test #7: Flash: 21 Td·s, Chromaticity (0.33, 0.33) at 2 Hz Background: 1100 Td, Chromaticity (0.33, 0.33)

Right Eye (Pupil 3.0 mm)

	a-wave		b-wave	
	ms	µV	ms	µV
1	14.5	-7.9	23.4	23.3
2	12.8	-7.8	23.5	19.6
	13.7	-7.8	23.5	21.5

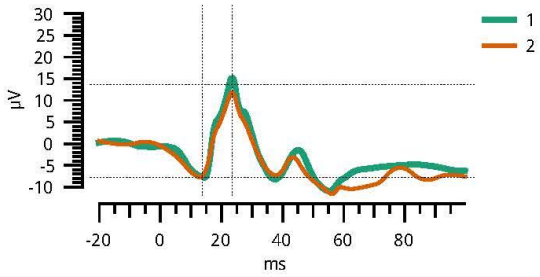

Left Eye (Pupil 2.7 mm)

	a-wave		b-wave	
	ms	µV	ms	µV
1	10.7	-4.5	23.5	22.4
2	13.5	-6.4	23.9	28.3
	12.1	-5.5	23.7	25.4

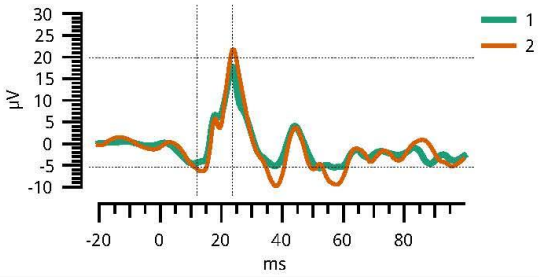

Test #8: Flash: 360 Td·s, Chromaticity (0.33, 0.33) at 2 Hz Background: 1100 Td, Chromaticity (0.33, 0.33)

Right Eye (Pupil 2.8 mm)

	a-wave		b-wave	
	ms	µV	ms	µV
1	11.2	-18.5	30.2	42.7
2	11.2	-12.0	29.9	41.3
	11.2	-15.3	30.1	42.0

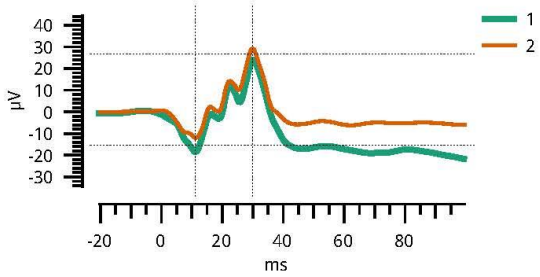

Left Eye (Pupil 2.5 mm)

	a-wave		b-wave	
	ms	µV	ms	µV
1	10.6	-6.9	30.0	25.2
2	9.7	-12.8	30.0	43.2
	10.1	-9.9	30.0	34.2

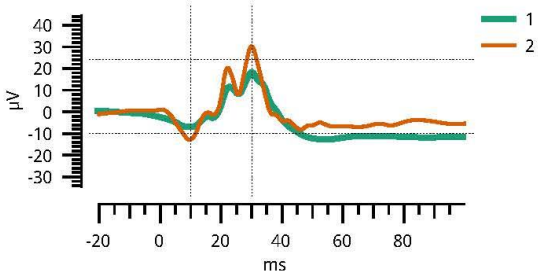

Patient ID: GA023
Birthdate: July 18, 2008
Test started: December 18, 2018, 4:31 PM
Report generated: December 18, 2018, 5:21 PM

Test #9: Flash: 12 Td·s, Chromaticity (0.33, 0.33) at 2 Hz Background: 1100 Td, Chromaticity (0.33, 0.33)

Right Eye (Pupil 2.5 mm)

	a-wave		b-wave	
	ms	µV	ms	µV
1	11.8	-5.2	21.9	11.9
2	14.5	-7.5	22.1	15.1
	13.2	-6.3	22.0	13.5

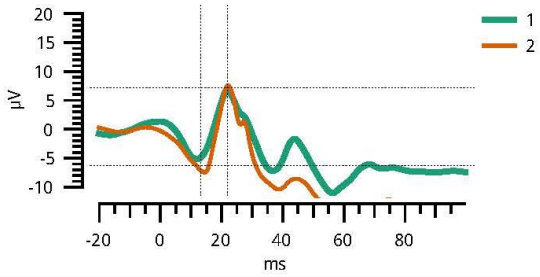

Left Eye (Pupil 3.2 mm)

	a-wave		b-wave	
	ms	µV	ms	µV
1	10.8	-5.0	21.8	16.9
2	14.6	-7.0	21.3	22.1
	12.7	-6.0	21.5	19.5

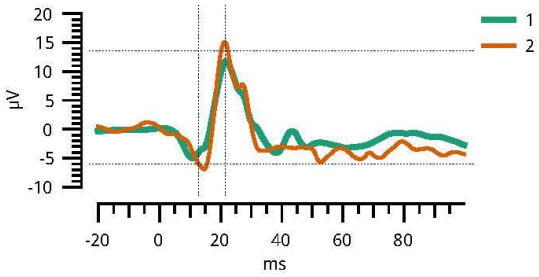

Test #10: Flash: 85 Td·s, Chromaticity (0.33, 0.33) at 2 Hz Background: 850 Td, Chromaticity (0.33, 0.33)

Right Eye (Pupil 3.0 mm)

	a-wave		b-wave	
	ms	µV	ms	µV
	9.2 ↔ 13.2	-1.7 ↔ -13.1	25.6 ↔ 30.6	14.6 ↔ 55.8
1	11.2 (50%)	-7.7 (63%)	28.5 (65%)	38.1 (69%)
2	11.0 (45%)	-7.8 (64%)	28.3 (60%)	38.0 (69%)
	11.1 (47%)	-7.7 (64%)	28.4 (63%)	38.0 (69%)

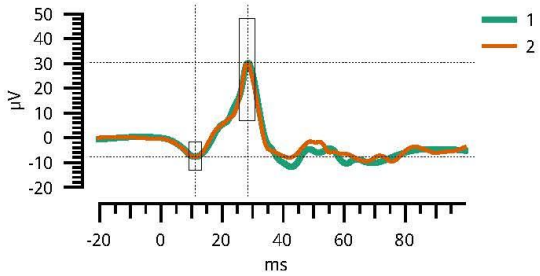

Left Eye (Pupil 2.6 mm)

	a-wave		b-wave	
	ms	µV	ms	µV
	9.2 ↔ 13.2	-1.7 ↔ -13.1	25.6 ↔ 30.6	14.6 ↔ 55.8
1	10.7 (34%)	-8.6 (74%)	28.0 (50%)	45.8 (88%)
2	12.7 (90%)	-11.1 (93%)	27.6 (35%)	39.1 (73%)
	11.7 (68%)	-9.8 (86%)	27.8 (43%)	42.4 (81%)

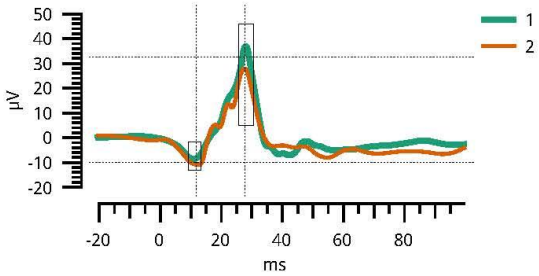

Table of ERG parameter results

Parameter	ASD Mean ± SE (95%CI)	Control Mean ± SE (95%CI)	*p*	*Multivariable effect size based the mixed model*	*Univariable effect size based t-tests at a flash strength*
Flash Strength 0.4 cd.s.m^{-2}					
a-wave time (ms)	14.0 ± 0.2 (13.7– 14.3)	14.0 ± 0.2 (13.7– 14.3)	.72	.00	.03
a-wave amplitude (µV)	3.6 ± 0.4 (2.8 – 4.4)	4.2 ± 0.4 (3.6 ± 5.1)	.030	-.12	-.18
b-wave time (ms)	22.3 ± 0.1 (22.1 -22.5)	22.1 ± 0.1 (21.9 – 22.2)	.06	.15	.14
b-wave amplitude (µV)	10.8 ± 1.4 (8.1 - 13.5)	12.3 ± 1.4 (9.5 - 15.1)	.13	-.08	-.28
b-wave : a-wave ratio	3.3 ± 0.2 (3.0 – 3.7)	3.3 ± 0.2 (3.0 – 3.6)	.97	.00	-.17
Flash Strength 0.8 cd.s.m^{-2}					
a-wave time (ms)	13.5 ± 0.2 (13.2 – 13.8)	13.5 ± 0.2 (13.2 – 13.9)	.75	.00	.06
a-wave amplitude (µV)	4.4 ± 0.4 (3.6 – 5.1)	4.7 ± 0.4 (3.9 – 5.5)	.20	-.06	-.12
b-wave time (ms)	23.4 ± 0.1 (23.3 – 23.6)	23.1 ± 0.1(21.9 – 22.2)	.005	.23	.32
b-wave amplitude (µV)	15.9 ± 1.4 (13.2 - 18.6)	17.0 ± 1.4 (14.3 – 19.8)	.25	-.06	-.20
b-wave : a-wave ratio	4.2 ± 0.2 (3.9 – 4.6)	4.1 ± 0.2 (3.8 – 4.4)	.52	.04	.04
Flash Strength 1.3 cd.s.m^{-2}					
a-wave time (ms)	12.9 ± 0.2 (12.6 – 13.2)	13.0 ± 0.2 (12.7 – 13.3)	.44	-.04	-.01
a-wave amplitude (µV)	5.1 ± 0.4 (4.4 – 5.9)	5.5 ± 0.4 (4.7 – 6.3)	.11	-.08	-.02
b-wave time (ms)	24.6 ± 0.1 (24.4 – 24.7)	24.3 ± 0.1 (24.1 – 24.5)	.007	.23	.34
b-wave amplitude (µV)	23.4 ± 1.4 (20.8 - 26.1)	25.8 ± 1.4 (23.0 – 28.5)	.012	-.13	-.32
b-wave : a-wave ratio	5.1 ± 0.2 (4.8 – 5.4)	5.1 ± 0.2 (4.8 – 5.5)	.69	.00	-.14
Flash Strength 2.5 cd.s.m^{-2}					
a-wave time (ms)	12.2 ± 0.2 (11.5 – 12.1)	12.4 ± 0.2 (12.1 – 12.7)	.19	-.08	-.04
a-wave amplitude (µV)	6.0 ± 0.4 (5.2 – 6.8)	6.6 ± 0.4 (5.8 – 7.4)	.016	-.11	-.21
b-wave time (ms)	26.2 ± 0.1 (26.1 – 26.4)	26.0 ± 0.1 (25.8 – 26.1)	.023	.15	.37
b-wave amplitude (µV)	30.1 ± 1.3 (27.4 – 32.7)	33.4 ± 1.4 (30.6 – 36.2)	<.001	-.19	-.38
b-wave : a-wave ratio	5.5 ± 0.2 (5.2 – 5.8)	5.6 ± 0.2(5.3 – 5.9)	.53	-.04	-.18
Flash Strength 4.0 cd.s.m^{-2}					
a-wave time (ms)	11.8 ± 0.2 (11.5 – 12.1)	12.0 ± 0.2 (11.7 – 12.3)	.11	-.08	-.06
a-wave amplitude (µV)	6.7 ± 0.4 (5.9 – 7.4)	7.4 ± 0.4 (6.6 – 8.2)	.002	-.13	-.27
b-wave time (ms)	27.5 ± 0.1 (27.3 – 27.6)	27.2 ± 0.1 (27.1 – 27.4)	.011	.23	.24
b-wave amplitude (µV)	31.4 ± 1.3 (28.7 – 34.1)	34.3 ± 1.4 (31.5 – 37.0)	.003	-.16	-.28
b-wave : a-wave ratio	5.2 ± 0.1 (4.9 – 5.5)	5.1 ± 0.2 (4.8 – 5.4)	.49	.05	.01
Flash Strength 6.3 cd.s.m^{-2}					
a-wave time (ms)	11.5 ± 0.2 (11.2 – 11.8)	11.6 ± 0.1 (11.3 – 11.9)	.13	-.05	-.03
a-wave amplitude (µV)	7.3 ± 0.4 (6.5 – 8.1)	8.2 ± 0.4 (7.4 – 9.0)	<.001	-.17	-.15
b-wave time (ms)	28.7 ± 0.1 (28.6 – 28.9)	28.4 ± 0.1 (28.3 – 28.6)	.002	.23	.39
b-wave amplitude (µV)	30.1 ± 1.4 (27.4 – 32.8)	31.9 ± 1.4 (29.2 – 34.7)	.044	-.10	-.17
b-wave : a-wave ratio	4.6 ± 0.1 (4.3– 4.8)	4.2 ± 0.2 (3.9 – 4.5)	.009	.19	.07
Flash Strength 8.9 cd.s.m^{-2}					
a-wave time (ms)	11.4 ± 0.1 (11.2 – 11.8)	11.6 ± 0.2 (11.3 – 11.9)	.30	-.10	-.13
a-wave amplitude (µV)	7.8 ± 0.4 (7.1 – 8.6)	8.8 ± 0.4 (8.0 – 9.6)	<.001	-.19	-.34
b-wave time (ms)	29.6 ± 0.1 (29.5 – 29.8)	29.3 ± 0.1 (29.1 – 29.4)	.019	.23	.32
b-wave amplitude (µV)	28.2 ± 1.3 (25.6 – 30.8)	29.6 ± 1.4 (26.9 – 32.4)	.12	-.08	-.21
b-wave : a-wave ratio	4.0 ± 0.2 (3.7 – 4.3)	3.5 ± 0.2 (3.2 - 3.8)	.001	-.02	.33
Flash Strength 13.0 cd.s.m^{-2}					
a-wave time (ms)	11.3 ± 0.2 (11.0 – 11.7)	11.4 ± 0.2 (11.1 – 11.7)	.68	-.04	-.13
a-wave amplitude (µV)	8.5 ± 0.4 (7.7 – 9.2)	9.5 ± 0.4 (8.7 – 10.3)	<.001	-.19	-.16
b-wave time (ms)	30.6 ± 0.1 (30.4 – 30.7)	30.1 ± 0.1 (30.0 – 30.3)	<.001	.38	.21
b-wave amplitude (µV)	26.5 ± 1.4 (23.8 – 29.1)	28.6 ± 1.4 (25.8 – 31.3)	.020	-.11	-.29
b-wave : a-wave ratio	3.5 ± 0.1 (3.3 – 3.7)	3.1 ± 0.2 (2.8 – 3.4)	.007	.19	.15

Flash Strength 16 cd.s.m^{-2}					
a-wave time (ms)	11.4 ± 0.2 (11.1 – 11.8)	11.4 ± 0.2 (11.1 – 11.8)	.94	.00	.08
a-wave amplitude (µV)	8.8 ± 0.4 (8.1 – 9.6)	9.9 ± 0.4 (9.1 – 10.7)	<0.001	-.21	-.31
b-wave time (ms)	30.9 ± 0.1 (30.8 – 31.1)	30.6 ± 0.1 (30.5 – 30.8)	<0.001	.23	.23
b-wave amplitude (µV)	26.4 ± 1.4 (23.7 – 29.0)	29.7 ± 1.4 (27.0 – 32.5)	<0.001	-.17	-.36
b-wave : a-wave ratio	3.3 ± 0.2 (3.0 – 3.6)	3.2 ± 0.2 (2.9– 3.5)	.52	.04	.10
Flash Strength 3.0 cd.s.m^{-2} ISCEV Standard					
a-wave time (ms)	11.6 ± 0.1 (11.4 – 11.8)	11.6 ± 0.1 (11.4 – 11.8)	.67	.00	.07
a-wave amplitude (µV)	6.6 ± 0.5 (5.6 – 7.6)	6.9 ± 0.6 (5.9 – 8.0)	.30	-.04	-.11
b-wave time (ms)	28.3 ± 0.1 (28.1 – 28.5)	28.2 ± 0.1 (28.1 – 28.4)	.72	-.05	-.13
b-wave amplitude (µV)	28.1 ± 2.6 (23.0 – 33.1)	29.5 ± 2.6 (24.4 – 34.7)	.24	-.04	-.11
b-wave : a-wave ratio	5.0 ± 0.2 (4.6 – 5.5)	4.5 ± 0.2 (4.0 – 4.9)	.06	.19	.14

Table 3 summary statistics for the ERG parameters across all flash strengths

RoC

AUC =0.74 for all participants

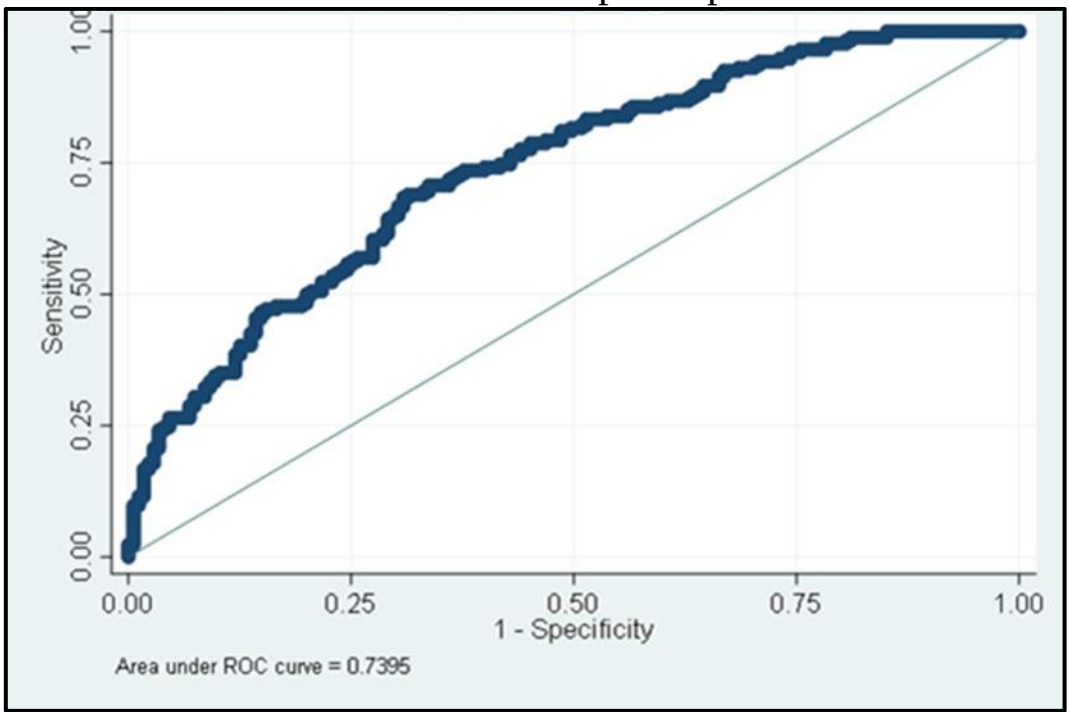

AUC =0.2 for all participants aged < 16 years of age

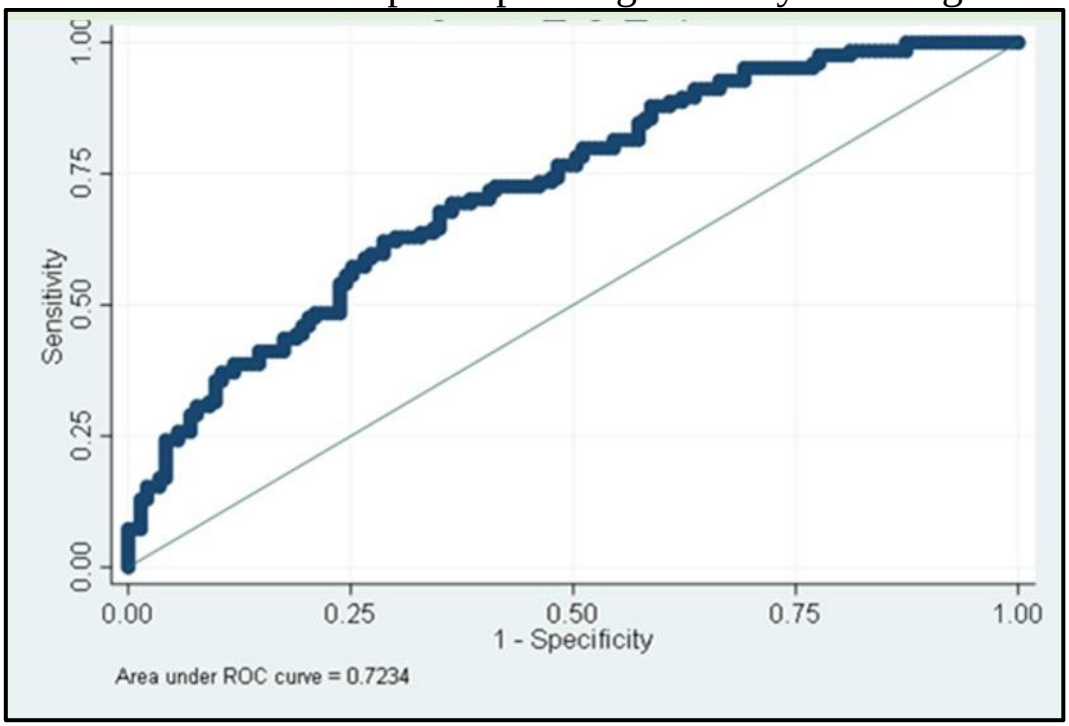

IRIS COLOR INDEX

Histogram showing the distribution of iris-color between the groups. The lower number is associated with lighter irises.

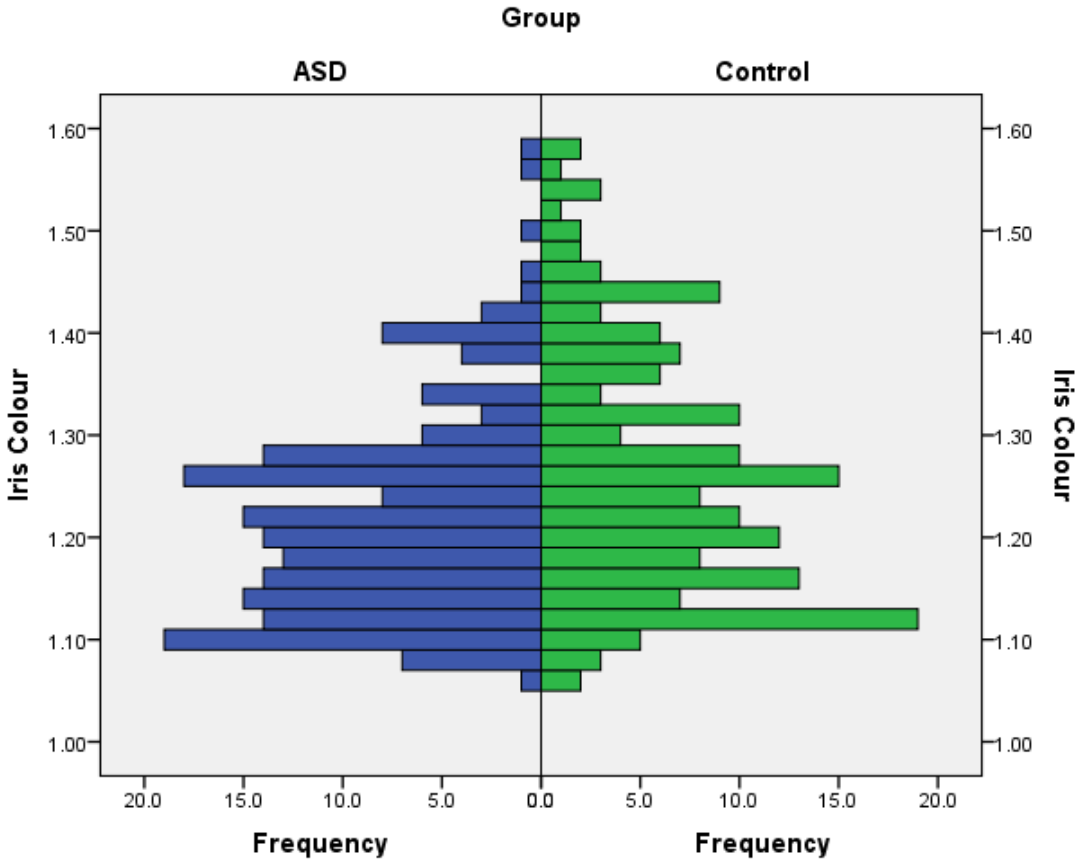

Histogram of distribution of iris colour in the ASD and Control group groups.